Frequency Shifts of a Quartz Crystal Microbalance Calculated with the Frequency-Domain Lattice-Boltzmann Method: Application to Coupled Liquid Mass

Diethelm Johannsmann[*1] and *Gunther Brenner*

[1]Institute of Physical Chemistry, Clausthal University of Technology, 38678 Clausthal-Zellerfeld, Germany

[2]Institute of Applied Mechanics, Clausthal University of Technology, 38678 Clausthal-Zellerfeld, Germany

The supporting information firstly reports certain steps of validation of the code. This concerns the form of the shear wave, the shifts of frequency and bandwidth induced by Newtonian liquids, tests of the Sauerbrey equation, and tests of the influence of finite grid resolution, finite height of the simulation volume, and finite ringing in-time. The second part of the supporting information contains the proof of Eq. 17 in the main text.

I Validation

I.1 Plane Shear Waves

The Newtonian liquid is the reference state for the large majority of QCM experiments concerned with questions from the life sciences. The baseline is acquired in buffer solution; all shifts of frequency and bandwidth are reported with respect to this baseline and the FD-LBM calculation must therefore capture this state well. Fig. S1 shows the real and the imaginary part of $u_E(x,z)$ achieved after 5 nanoseconds (A and B) and after 1000 nanoseconds (C and D) of ringing-in. The wave is launched at the left-hand side of the cell. After 1000 ns, the steady state has been reached. In this state, the waves decay towards large z because of viscous dissipation. Panel E shows the real part of the steady-state solution with a particle adsorbed to the center of cell. The particle is rigidly coupled to the sensor surface. The velocity therefore is equal to unity inside the particle. One observes the expected distortion of the flow outside the particle. Panel F shows the area-averaged in-phase component of the steady-state of the semi-infinite fluid together with the analytical result, which is

$$u(z,t) = \mathrm{Re}\left(\exp\left(-\frac{1+i}{\delta} z \right) \right) \exp(\mathrm{i}\omega t) = \cos\left(\frac{z}{\delta} \right) \exp\left(-\frac{z}{\delta} \right) \exp(\mathrm{i}\omega t) \qquad \text{Eq. 1}$$

* author for correspondence, electronic mail: johannsmann@pc.tu-clausthal.de

$\delta = (2\eta/(\rho\omega))^{1/2}$ is the penetration depth. The numerical and the analytical result can hardly be distinguished in the graph. The dashed blue line shows the residual expanded by a factor of 100.

The most important quantitative measure of numerical accuracy is the frequency shift. Equating the load impedance in Eq. 1 in the main text with the shear wave impedance of the Newtonian liquid, one finds[1]

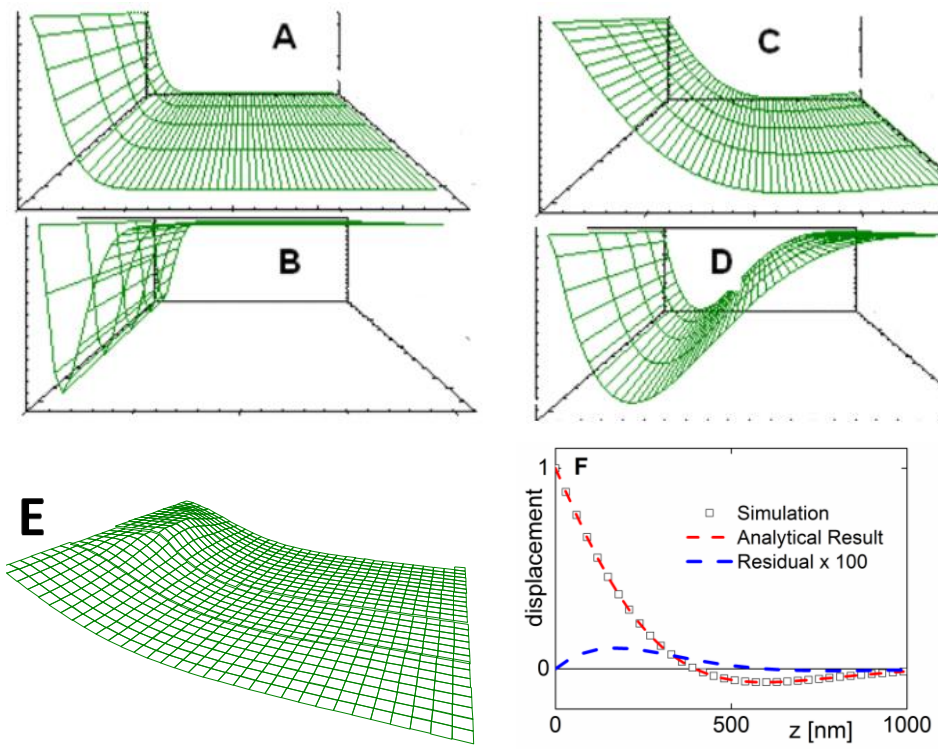

Fig. S1: Panels A–D and F: Solutions to the problem without adsorbed particles. Panel: E: Solution with an adsorbed hemisphere in the center. The grid resolution is Δr = 30 nm; the cell height is h_C = 1 µm. The ordinate shows the real part of the tangential velocity (along x); the two other axes are a cut through the simulation volume along the xz-plane. Panels A, C, E, and F show the real part of u_E, panels B and D show the imaginary part. At a time of 5 ns after the excitation was turned on (A and B), the shear wave is confined to a range close to the resonator surface (to the left). The boundary condition at this surface is $u_E(z = 0) = (1 + 0i)$. After a microsecond of simulation time (C and D), the steady state has been reached. Panel F shows the real part of $u_E(z)$ in the steady state together with the analytical result from Eq. 1. The fractional deviation of the simulation from Eq. 1 is about 10^{-3}.

Eq. 2

$$\frac{\Delta f + \mathrm{i}\Delta\Gamma}{f_0} = \frac{\mathrm{i}}{\pi Z_q} Z_{liq} = \frac{\mathrm{i}}{\pi Z_q}\sqrt{\mathrm{i}\omega\rho\eta} = \frac{-1+\mathrm{i}}{\sqrt{2}\pi Z_q}\sqrt{\omega\rho\eta}$$

Δf and $\Delta\Gamma$ are of equal magnitude and opposite sign. Inserting values, one finds $-\Delta f = \Delta\Gamma = 716.8$ Hz. The simulation results are $\Delta f = -716.4$ Hz and $\Delta\Gamma = 717.2$ Hz. There is a systematic error of 0.6 Hz. 0.6 Hz may appear to be a small number compared to the absolute value, but the adsorbates of interest in experiment induce frequency shifts in just that range. The precision of the modern QCMs actually is slightly better.

I.2 Frequency Shift at Full Coverage

The Sauerbrey equation (Eq. 3 in the main text) is strictly correct even in liquids as long as the sample is a thin, laterally homogeneous, and perfectly rigid layer. The results of this test are shown in Fig. S2. The sample was a rigid, laterally infinite sheet of variable thickness, placed onto the resonator surface. The main deviation between the simulation results and the Sauerbrey equation (dotted line) is caused by the finite resolution of the grid, which was $\Delta r = 0.25$ nm. The resolution can be improved, in principle, but both the memory space and the simulation time scale as Δr^{-3}.

At this point, one needs to remember that the FD-LBM scheme calculates the geometric thickness, while the QCM determines the mass per unit area (see end of section SII). If the density of the protein is different from the density of water, a correction factor must be applied. Annexin 5 actually is slightly more dense than water, but the correction was still omitted in S2.

I.3 Effects of Finite Grid Size, Finite Cell Height, and Finite Ringing-in Time

Fig. S3 collects results on how the finite resolution of the lattice, and the finite height of the cell, and the finite time for ringing-in affect the derived frequency shifts. As panel A shows, the finite grid resolution is the most critical issue. The office PCs used for these calculations can afford grids with about 10^6 sites. Of course more advanced computers can improve on this number, but given that memory and computation

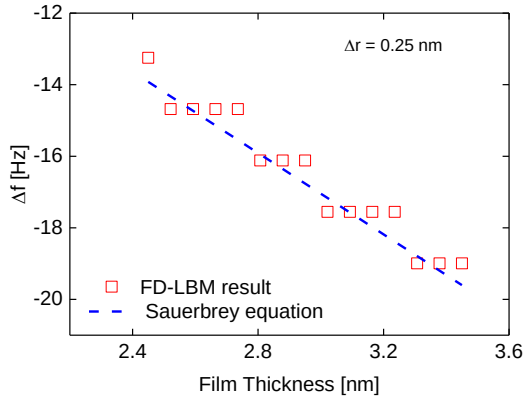

Fig. S2 Frequency shifts induced by the presence of a thin rigid film of variable thickness. The simulation cannot resolve geometric details beyond the grid-resolution, which was $\Delta r = 0.25$ nm. In all other regards, the Sauerbrey equation is reproduced.

time scale as Δr^{-3}, the grid resolution will be a critical constraint, even if parallel computing is implemented. Typical dimensions employed here were a grid resolution of Δr = 0.25 nm, a cell height of h_C = 10 nm (40 lattice units) and width of w_C = 30 nm (120 x 120 lattice units). With a particle radius of 2.7 nm, a cell width of 30 nm corresponds to a coverage of 2.5% if the cell contains one particle only. It is stated in the results section that the particles were randomly placed onto the resonator surface. Random sequential adsorption was of course limited to the area of the cell. At larger scales, the pattern of adsorbed spheres is periodic, following from the periodic boundary conditions at the side of the simulation cell.

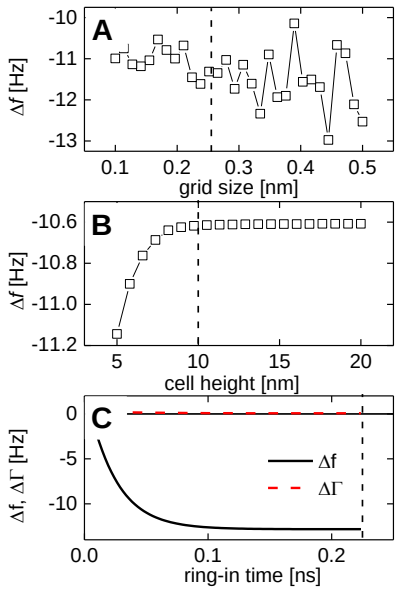

Fig. S3: Dependence of the frequency shift on the resolution of the grid (A), the height of the cell (B), and the ringing-in time (C). The cell width was 9 nm. One particle was adsorbed to the center of the cell, which amounts to a coverage of 30%.

With cell dimensions of 30 x 30 x 10 nm and a maximum of 10^6 lattice sites, the resolution of the grid cannot be lower than about 0.1 nm. A resolution of Δr = 0.25 nm was the default value. As Fig. S3A shows, this setting leads to uncertainties in the absolute values of Δf of the order of 10%. This uncertainty becomes important, when interparticle distances are changed. For that reason, the simulations leading to Figs. 5 and 7 in the main text were repeated and averaged 10 times with variable, randomly chosen particle positions. The uncertainty resulting from finite grid resolution does not affect the comparison of Δf and $\Delta\Gamma$. Neither does it affect the comparison between overtones (Fig. 4 in the main text).

Compared to grid resolution, finite cell height is less critical (Fig. S3B). The difference between values of Δf obtained at h_C = 20 nm and h_C = 10 nm is 0.02 Hz, which amounts to an error of about 2%. A frequency shift of 0.02 Hz is close the limit of detection of the modern QCMs. The simulation time scales as the cubic power of h_C. There is a first linear dependence on h_C because the number of cells in the simulation volume scales as h_C and a second quadratic dependence, because the ringing-in time scales as h_C^2/ν (ν the kinematic viscosity). Given the cubic dependence, lowering h_C and accounting for non-planar flow with the methods discussed in Ref. 2 presumably is worthwhile.

The dependence of Δf on ringing in-time is even less critical (Fig. S3C). The difference in Δf between a ringing-in time of 0.15 ns and 0.22 ns was 0.02 Hz. Since the total time of computation scales linearly with ringing-in time, adapting the ringing-in time to the desired accuracy is inexpensive.

II Appendix: Derivation of Eq. 17

Eq. 17 applies to samples, which are acoustically thin and are structured on a scale much below the wavelength of sound. Such layers can be modeled as effective media, that is, can be represented as thin, homogeneous layers with an effective mass per unit area, m_f, and an effective acoustic impedance, Z_f. Thin layers of this kind lead to a one-to-one relation between the amplitude of the wave reflected back to the resonator surface from the film-bulk interface, u_r, and the amplitude of the wave transmitted across this interface, which eventually reaches the outer boundary of the simulation cell, u_t (Fig. S4). Since there is no wave reflected from the upper boundary at $z = L$, u_t is equal to u_{upb} from Eq. 17 in the main text.

The amplitude of the reflected wave governs the load impedance, Z_L, following the relation

$$Z_L = \frac{\sigma_{xz}}{u_{tot}} = Z_f \frac{u_0 - u_r}{u_0 + u_r} \qquad \text{Eq. 3}$$

u_0 is the amplitude of the wave launched by the oscillating surface. Once the amplitude u_r is known, the frequency shift can be calculated from the small-load approximation (Eq. 1 in the main text).

The primary wave is of the form of $u_0\exp(-ik_f z))$ with k_f the wavenumber inside the film. ($u_0 + u_r$ is normalized to unity, not u_0.) The amplitude reflection coefficient at the film-liquid interface is

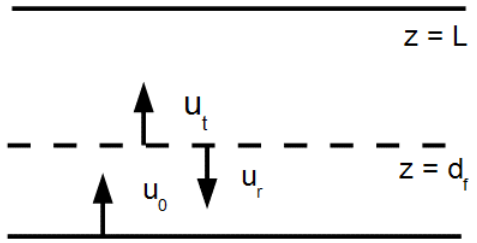

Fig. S4: Geometry and definitions of variables underlying the calculation leading to Eq. 17 in the main text. Since the sample is acoustically thin, it may be represented as a planar layer of thickness d_f. The stress at the resonator surface follows from the amplitudes u_0 and u_r. Unfortunately, u_r cannot not be determined with sufficient accuracy using the bounce-back scheme. *If the layer is acoustically thin, there is one-to-one relation between u_r and u_t,* where the latter is amplitude of the wave transmitted to beyond the interface of the sample. The amplitude u_t *can* be extracted with sufficient accuracy from the stress at the outer boundary of the simulation volume at $z = L$. Using the relation between u_r and u_t, one translates the amplitude u_t to an equivalent amplitude u_r and calculates Δf from this value of u_r.

Eq. 4

$$r_{f,liq} = \frac{Z_f - Z_{liq}}{Z_f + Z_{liq}}$$

Z is the shear-wave impedance; the indices f and liq denote the film and the liquid, respectively. u_r evaluated at the resonator surface takes the form

Eq. 5

$$u_r = \exp\left(-2\mathrm{i}k_f d_f\right)\frac{Z_f - Z_{liq}}{Z_f + Z_{liq}}$$

d_f is the thickness of the film. Inserting u_r from Eq. 5 into Eq. 3 and Taylor-expanding the result to first order in d_f leads to[3]

Eq. 6

$$Z_L \approx \mathrm{i}\omega\rho_f d_f\left(1 - \frac{Z_{liq}^2}{Z_f^2}\right) + Z_{liq}$$

The relation $k = \omega/(\rho Z)$ was used in the derivation. We define Δf as being referenced to the state, where the resonator is immersed in the liquid with no film present. In this state, we have $Z_L = Z_{liq}$, which means that Z_{liq} must be subtracted from the load impedance in the calculation of Δf. We arrive at[4]

Eq. 7

$$\frac{\Delta f + \mathrm{i}\Delta\Gamma}{f_0} \approx \frac{\mathrm{i}}{\pi Z_q}\omega\rho_f d_f\left(1 - \frac{Z_{liq}^2}{Z_f^2}\right)$$

The amplitude transmission coefficient at the film-liquid interface is

Eq. 8

$$t_{f,liq} = \frac{u_t}{u_0} = \frac{2Z_{liq}}{Z_f + Z_{liq}}$$

The amplitude of the transmitted wave at the outer boundary of the cell (at $z = L$) is

Eq. 9

$$u_t = \exp\left(-\mathrm{i}k_f d_f\right)\frac{2Z_{liq}}{Z_f + Z_{liq}}\exp\left(-\mathrm{i}k_{liq}\left(L - d_f\right)\right)$$

There are two complications. Firstly, the amplitude u_t as determined in the simulation is referenced to $u_0 + u_r$ (not to u_0). u_r depends on Z_f and d_f, as well. Secondly, one cannot just ignore the film in the reference state because the definition the amplitudes depends on the impedance of the material at the respective location. For a discussion see Ref. 5. As a consequence, one needs to consider the limit of $d_f \to 0$ (but not $Z_f \to Z_{liq}$) of Eq. 9 in order to calculate u_t in the reference state.

Normalizing u_t from Eq. 9 to the velocity at $z = 0$ (which is u_0+u_r) and expanding the result to first order in d_f, one finds

Eq. 10

$$\frac{u_t}{u_0 + u_r} \approx \exp\left(-\mathrm{i}k_{liq}L\right)\left(\frac{Z_{liq}}{Z_f} + \frac{\mathrm{i}\omega\rho_{liq}d_f}{Z_f}\left(\frac{\rho_f}{\rho_{liq}} - \frac{Z_{liq}^2}{Z_f^2}\right)\right)$$

In the limit of $d_f \to 0$ one has

Eq. 11

$$\frac{u_{t,ref}}{u_0 + u_r} \approx \exp\left(-\mathrm{i}k_{liq}L\right)\frac{Z_{liq}}{Z_f}$$

which leads to

Eq. 12

$$\frac{u_t}{u_{t,ref}} - 1 \approx \frac{\mathrm{i}\omega\rho_f d_f}{Z_{liq}}\left(1 - \frac{\rho_{liq}Z_{liq}^2}{\rho_f Z_f^2}\right)$$

At this point, we need the assumption $\rho_{liq} \approx \rho_f$. If the two densities are similar (which they often are in soft-matter experiment) the comparison of Eq. 7 and Eq. 12 leads to

Eq. 13

$$\frac{\Delta f + \Delta \mathrm{i}\Gamma}{f_0} \approx \frac{\mathrm{i}}{\pi Z_q} Z_{liq} \left(\frac{u_t}{u_{t,ref}} - 1 \right) = \frac{\mathrm{i}}{\pi Z_q} Z_{liq} \left(\frac{u_{upb}}{u_{upb,ref}} - 1 \right)$$

One can phrase the consequences of the assumption $\rho_{liq} \approx \rho_f$ in a different way: The QCM applied to Sauerbrey-type layers measures the apparent mass per unit area, not the geometric thickness. The density must be known in order to convert mass to thickness. With FD-LBM simulations, it is the other way round: the FD-LBM method predicts the effective thickness and the density must be known in order to convert the thickness to an effective mass.

References

1 Borovikov, A. P., Measurement of Viscosity of Media by Means of Shear Vibration of Plane Piezoresonators. *Instruments and Experimental Techniques* **1976,** 19, (1), 223-224.

2 Mecke, K. R., Thermal fluctuations of thin liquid films. *Journal of Physics-Condensed Matter* **2001,** 13, (21), 4615-4636.

3 Johannsmann, D., *The Quartz Crystal Microbalance in Soft Matter Research: Fundamentals and Modeling*. Springer: 2014.

4 Johannsmann, D., Viscoelastic analysis of organic thin films on quartz resonators. *Macromolecular Chemistry and Physics* **1999,** 200, (3), 501-516.

5 Lekner, J., *Theory of Reflection of Electromagnetic and Particle Waves*. Springer: 1987.